Evolution and Geology of Eburru-Badlands Geothermal Prospect— Central Kenyan Rift

Irene Ronoh

Kenya Electricity Generating Company (KenGen)
ironoh@kengen.co.ke

Keywords

Exploration, geology, Eburru-Badlands, Scanning Electron Microprobe, classification, bulk rock chemistry, peralkaline, subalkaline, evolution

ABSTRACT

Eburru-Badlands Geothermal Field is characterized by Trachyte, Pantellerites, Basalts and Pyroclastics. The lavas are classified into pre- and post- faulting events estimated to be aged between 1.2 Ma and 100 years BP. The older formations are affected by a major faulting event dated between 0.8 Ma and 0.4 Ma (Clarke et al., 1990). The younger lavas include Trachyte (Et2), basalt (Eb2), Pyroclastic (Ep2) and Pantellerite (Ep2). They are not faulted and occur along the younger N-S faults. Thirteen rock samples from surface outcrops were analyzed and identified as Trachyte (Et1), Trachyte (Et2), Basalt (Eb2), Pyroclastic (Ep2) and Pantellerite (Ep2). The Trachyte (Et1) is folded and fractured, and hence belongs to the pre-faulting stratigraphic sequences. The rocks are porphyritic with quartz, sanidine, pyroxenes, amphiboles, plagioclase and olivine of varying amounts. Classification of these rock units indicates that SiO_2 weight percent increases from basalts (45-50%) through Trachyte (65%) and Pantellerites (69-74%) to Pyroclastics (78%). The Pyroclastic rocks (Ep2) are mainly obsidian flows which are devitrified and appear brecciated. High (Na_2O+K_2O) weight percent content in Trachytes and Pantellerites makes them strongly peralkaline. The silicic rocks are characterized by low Al_2O_3 and Fe_2O_3. Basalts are associated with an increase in Al_2O_3 and with a decrease in SiO_2. Analyzed basaltic and Pyroclastics samples are subalkaline.

Geochemical models of basalts and silicic peralkaline lavas show that the magmas are ultimately mantle-derived and that the evolution was dominated by fractional crystallization processes. This classification shows an evolution trend from basalts through Trachyte to Pantellerite.

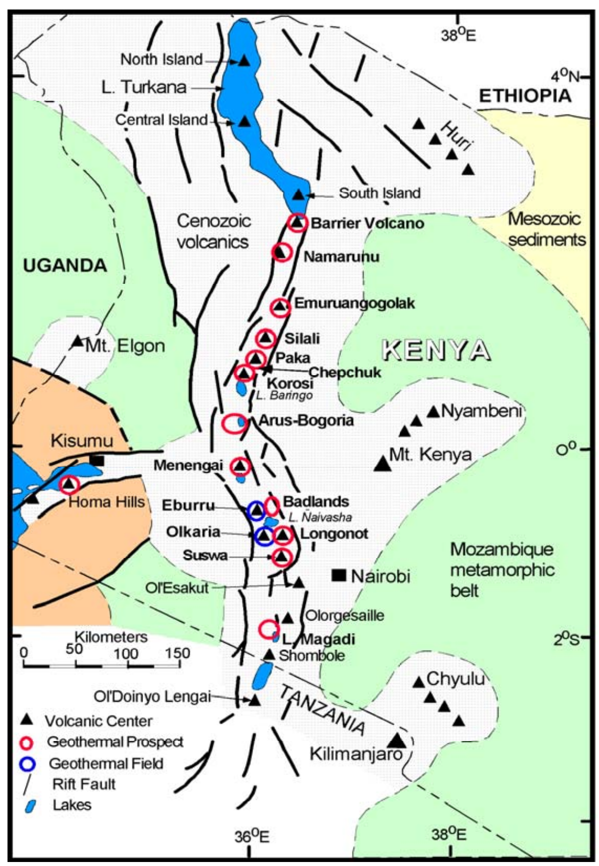

Figure 1. Location map of Eburru-Badlands area in the Central Kenyan Rift, modified from Mariita (2009).

1. Introduction

Eburru-badlands geothermal prospect is located within southern central Kenyan rift and is situated 20 km north of Olkaria Geothermal Field (Figure 1). Eburru volcanic centre has an inferred caldera marked by alignment of craters and is structurally connected to the badlands area extending to the north of the caldera. Currently, surface exploration studies are on-going to map the area outside the Eburru Volcanic Centres in order to determine if the resource extends to the Badlands area and to understand the evolution of both fields.

The objective of this study is to analyse the rock samples collected during surface structural mapping so as to characterize and understand the compositional variations and the evolution of the Eburru-Badlands lavas.

2. Geology and Stratigraphy of Eburru-Badlands Area

The geology of Eburru Volcanic Complex is associated with Pleistocene to Holocene volcanism that underwent four stages of evolution (Clark et al., 1990). Lavas in the area were formed from the Pre- and Post-faulting events as summarized in Table 1.

Table 1. Generalized stratigraphy of Eburru-Badlands geothermal area (Clarke et al, 1990).

Age		Stratigraphic unit	Description
0.4 Ma – 100yr BP	Oldest-Youngest	Younger Pantellerite Er2	Overlay younger Pyroclastics Ep2
		Younger Pyroclastics Ep2	East and West of Eburru
		Younger Basalts Eb2	Badlands-overlay older Basalt Eb1
		Younger Trachyte	Overlay older Pyroclastic Ep1
0.8 Ma – 0.4 Ma		Faults	N-S faults cuts the older formations
1.2 Ma – 0.4 Ma	Oldest-Youngest	Older Pyroclastics Ep1	Caps older Trachyte Et1
		Older Basalt Eb1	Badlands –formed same time as older Trachyte Et1
		Older Trachyte Et1	NW and East of Eburru
		Older Pantellerite Er1	Western Massif

Structural Setting

The tectonic setting of Eburru-Badlands Geothermal Field has been studied extensively and reported by many authors. Omenda and Karingithi (1993) established that Eburru volcanic zone consists of east and west volcanic centres occurring as curve-linear structures. The two ring structures are located at the centre of Eburru area. The rift forming faults trend NNW-SSE while the rift floor faults in the central sector, some of which cut through Eburru, trend in N-S and NNE-SSW direction, (Figure 2). Along the main faults that occur on the mountain, many phreatic and phreatomagmatic craters occur. Some of the craters form a circular structure that is interpreted to be margins of a buried caldera.

Grabens and mini-grabens are marked by large open fractures and faults common on the eastern Eburru Volcano. Cinder cones are found within the mini-graben structures. Intense volcanic eruption and up-doming resulted in a series of dykes, noted in Badlands. They include active fumaroles, altered, hot and steaming ground, geothermal grass (*Fimbristylis Exillis*) cover (in regions of 40-55^{o}C) and hydrothermal deposits. The fumaroles show the highest temperature recorded in the area (95.3^{o}C).

Sample Collection and Methodology

The purpose of the fieldwork was to map and verify geologic structures and contacts on a geological base map earlier prepared by Clarke et al., in 1990. Samples were collected and analyzed to confirm if detailed geological mapping is required to confirm the rock units mapped earlier.

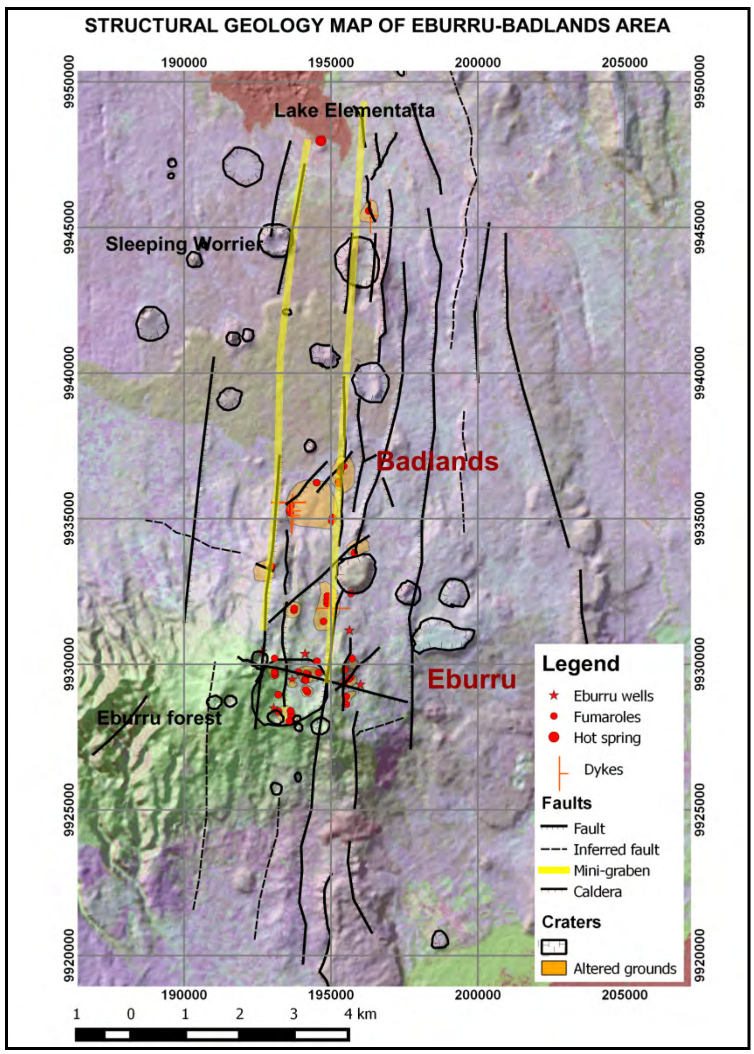

Figure 2. Structural map of Eburru-Badlands area (Kandie, 2014).

Thirteen representative samples were chosen for different geological analyses at the University of Auckland laboratories. Most of the samples were collected on the northern parts of the Eburru Caldera which less mapped by the earlier explorers. Rock sampling points shown in Figure 3.

The analytical methods used during the study are:

1. Petrographic analysis
2. X-ray Diffractometer (XRD) for whole rock analysis
3. X-ray Fluorescence (XRF) for analysis of major oxides and selected trace elements
4. Scanning Electron Microprobe (SEM)

3. Results

3.1 XRD Bulk Rock Analyses

Results from whole rock chemistry indicate that the major phenocrysts are alkali feldspars, quartz ± pyroxenes ± plagioclase ± olivine. Amphiboles and anorthoclase present in some samples.

Petrography and Scanning Electron Microprobe (SEM) Analyses

Structural characteristics of the rocks were determined from these analyses. Pyroclastic rock is composed of phenocrysts of sanidine and large amounts of quartz. Amphiboles and pyroxenes were also noted. Groundmass accounts for 60% of the rock.

Pantelleritic lavas are phyric with phenocrysts between 15% and 25%, mainly composed of quartz, sanidine, pyroxenes (aegirine + hedenbergite ± augite). Vesicle infillings with chlorite and amorphous silica, see Figure 4.

Trachytic samples have phenocrysts that vary in content between 1.5% and 7% and are mainly composed of sanidine, pyroxenes (aegirine + hedenbergite), aenigmatite, and anorthoclase with varying percentages. Matrix is feldspar-rich, glassy ± quartz, with trachytic flow texture observed in Figure 4c and 4d. Sample GP1-14 is highly folded and appears brecciated.

Basalts are porphyritic with plagioclase feldspars dominating the groundmass (about 30%). Olivine, sanidine and pyroxenes (hedenbergite) are embedded in a fine grained to glassy matrix. Rocks show varying densities but there are few vesicles with clay infillings.

Primary minerals like feldspars and olivine show crystal fracturing and slight alteration along the planes. Alteration is characterized mainly by clays (chlorite) in veins and vesicles, (Figure 5). A possible occurrence of amorphous silica is noted from nodular grains observed in the vesicles, (Figure 5c).

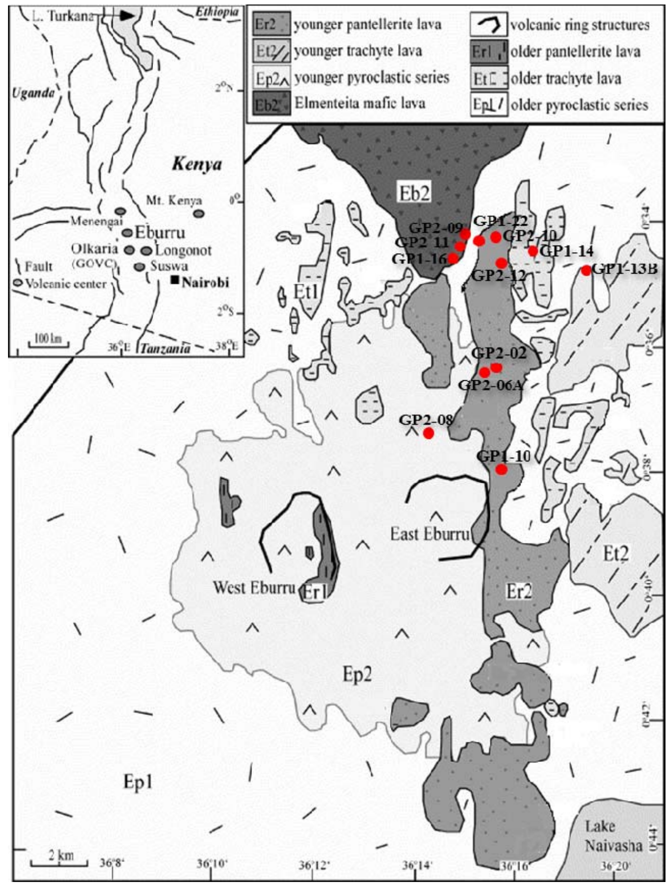

Figure 3. Map showing sampling points in Eburru-Badlands area, modified from Omenda et al., (2006).

Table 2. Whole rock XRD data of Eburru-Badlands samples.

Sample no.	Major	Minor	Rock type
GP2-02	Sanidine, quartz	Na-feldspar	Pantellerite (Er2)
GP2-6A	Sanidine, quartz	Na-feldspar	Pantellerite (Er2)
GP2-6B	Sanidine, quartz		Pantellerite (Er2)
GP2-08	Quartz, sanidine	K-feldspar,	Pyroclastics (Ep2)
GP2-09	Plagioclase (anorthite), hedenbergite, olivine (fayalite)	Aegirine, sanidine	Basalt (Eb2)
GP1-10	Quartz, k-feldspars, augite	Sanidine, plagioclase, olivine (fayalite)	Pantellerite (Er2)
GP2-10	Quartz, Na-feldspar	Sanidine, plagioclase, amphibole (arfvedsonite)	Pantellerite (Er2)
GP2-11	Anorthite, sanidine, olivine	Hedenbergite, augite	Basalt (Eb2)
GP2-12	Quartz, hedenbergite, aegirine, sanidine	Plagioclases, K-feldspars	Pantellerite (Er2)
GP1-13B	Sanidine, aegirine	Hedenbergite, quartz	Trachyte (Et2)
GP1-16	Plagioclase (anorthite), olivine		Basalt (Eb2)
GP1-22	Quartz, sanidine	Amphibole (arfvedsonite), aegirine	Pantellerite (Er2)
GP1-23	Quartz, sanidine, K-feldspar	Olivine (fayalite), anorthoclase	Pantellerite (Er2)

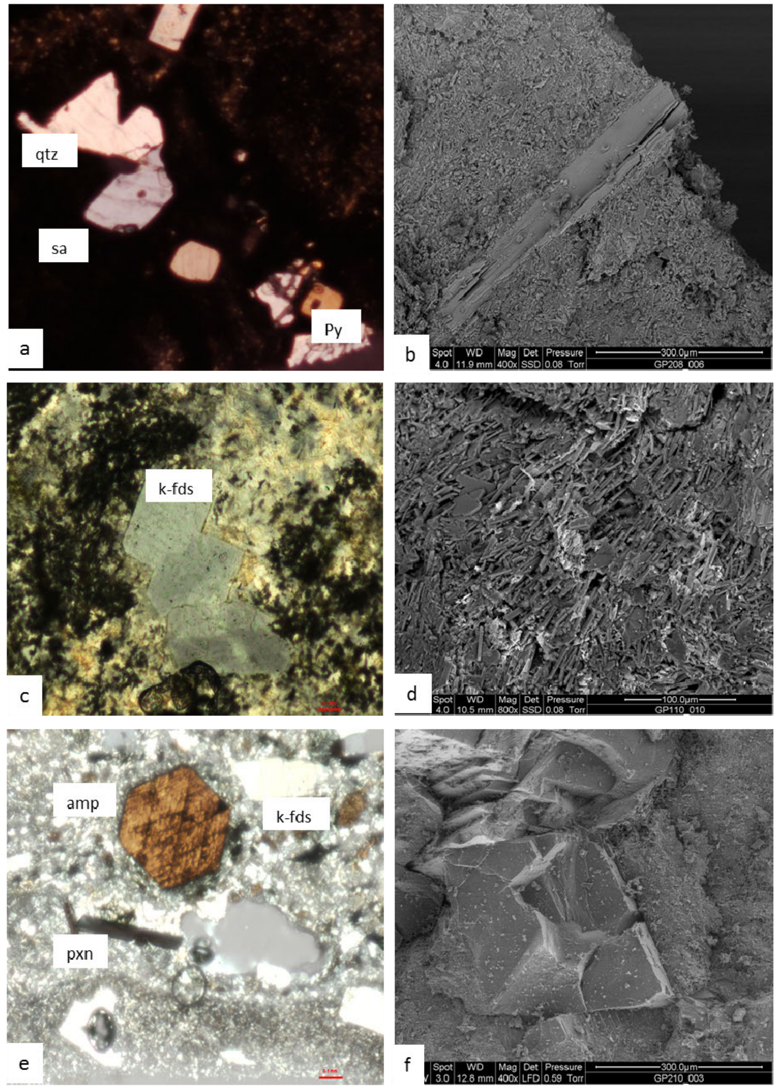

Figure 4. a) Pyroclastic unit with quartz (qtz), sanidine (sa) and pyrite (py); b) photomicrograph of pyroxene (aegirine/augite); c) cluster of k-feldspars in trachyte d) photomicrograph showing flow texture in a trachyte sample; e) amp (arfvedsonite), pxn (pyroxene); f) photomicrograph of an amphibole in a pantellerite.

Petrographic and SEM analyses give a good relationship between groundmass and the phenocrysts' content with most rocks being porphyritic with fine-grained to glassy matrix.

Alteration of feldspars to clays is noted in sample GP2-10 as shown in the Energy Dispersive X-Ray (EDX) Spectrum in Figure 6.

XRF Analysis Results

By plotting the analyzed rock units on a Total Alkali Silica (TAS) diagram (Le Bas et al. 1986), pantellerites plot in the stability field of rhyolites and show a range of silica content indicative of highly evolved magma composition. Trachyte has high silica concentrations, and hence plots close to the boundary between trachytes and rhyolites while one pyroclastic sample displays the highest silica and low alkali composition compared to pantellerites (Figure 7). Basalts have low silica and alkali content. The high total alkali content of the pantellerites is high, hence pantellerites noted to be strongly peralkaline. The pyroclastic and basaltic units are sub-alkaline. Normalized major oxides of the analyzed Eburru-Badlands samples, (Table 3).

Basalts are characterized by high Al_2O_3 and Fe_2O_3 of about 13-15% while trachytes and pantellerites have low concentrations of Al_2O_3 (8- 10%), Fe_2O_3 (7-11%), CaO (0.3-1.4%), MgO (0.05-0.49%), P_2O_5 (<0.05%), and TiO_2 (0.3-0.8%). A correlation of the major elements shows an increase in Al_2O_3 and Fe_2O_3 with decrease in SiO_2 in the samples, (Figure 8).

The trace element data for Eburru-Badlands trachytes, basalts and pantellerite (Table 4) shows that, apart from basalts, the rocks are highly depleted with respect to compatible elements (V, Cr, Sr, Co, Ni and Ba). The incompatible elements show an increase in concentrations from basalts, trachytes to pantellerites, (Figure 9).

The variation in trace elements in the rock samples as shown in Table 3 displays a systematic increase in incompatible elements (Zr, Nb, Y and Rb) from basalts through trachyte to pantellerite, and decrease of compatible element concentrations (Co, Ni, Sr, Cr, V and Ba) indicating a close magmatic relationships between the rocks.

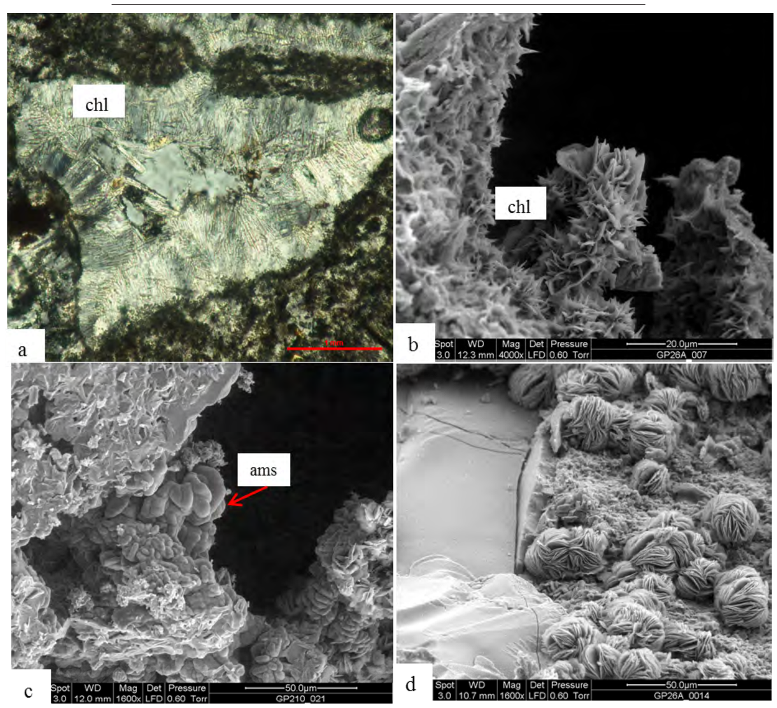

Figure 5. Chlorite and opal infilling vesicles and veins; chl (chlorite), ams (amorphous silica).

4. Discussion and Conclusion

Eburru Volcanic Complex is formed of trachytes, pantellerites, pyroclastic deposits and basaltic units to the north of the Eburru crater. Older formations are faulted. Analyzed sample GP1-14 appears highly folded, which could be as a result of faulting. Younger formations occur along the N-S trending faults and are not faulted which indicate a post- faulting occurrence.

Analyzed rocks have phenocryst assemblages containing quartz, sanidine, pyroxenes (hedenbergite, aegirine/augite), amphibole (arfvedsonite), plagioclase, k-feldspars and fayalite.

Rock chemistry was confirmed by Total Alkali Silica (TAS) diagram (Figure 7), where pantellerites and pyroclastics have high silica content (>69%) and plot on the rhyolites' stability field indicating the most evolved composition. Trachyte has silica content (65%) higher than basaltic units and plots next to the boundary between trachytes and rhyolites. Basalts show small variations in silica content (47-50%).

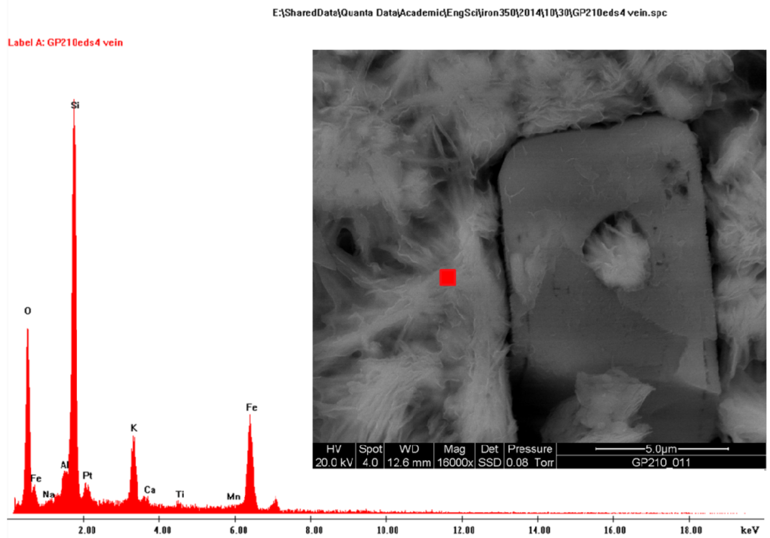

Figure 6. Photomicrograph of chlorite close to a feldspar crystal (red box indicate the EDX analyzed section).

Table 3. Major element data for Eburru-Badlands samples.

Rock sample (% Oxides)	2	8	13B	9	16	12	10	22	23
SiO_2	72.46	78.1	65.15	49.06	47.45	73.25	73.86	71.74	69.56
Al_2O_3	9.99	8.34	10.14	14.51	14.89	9.6	8.69	9.24	10.05
Fe_2O_3	7.51	6.44	11.82	13.19	14.32	7.11	7.79	8.75	11.44
MgO	0.08	0.07	0.49	5.91	6.38	0.07	0.06	0.16	0.12
P_2O_5	0.01	0.02	0.05	0.47	0.59	0.02	0.01	0.02	0.02
MnO	0.12	0.08	0.38	0.21	0.22	0.19	0.13	0.23	0.4
CaO	0.32	0.24	1.34	9.96	9.88	0.68	0.35	0.33	0.83
Na_2O	4.68	2.92	5.41	3.38	2.87	4.32	4.29	4.9	3.63
K_2O	4.48	3.49	4.41	1.1	0.77	4.5	4.53	4.32	4.28
TiO_2	0.36	0.3	0.81	2.21	2.63	0.27	0.29	0.3	0.36
Total	100.	100	100	100	100	100	100	100	100

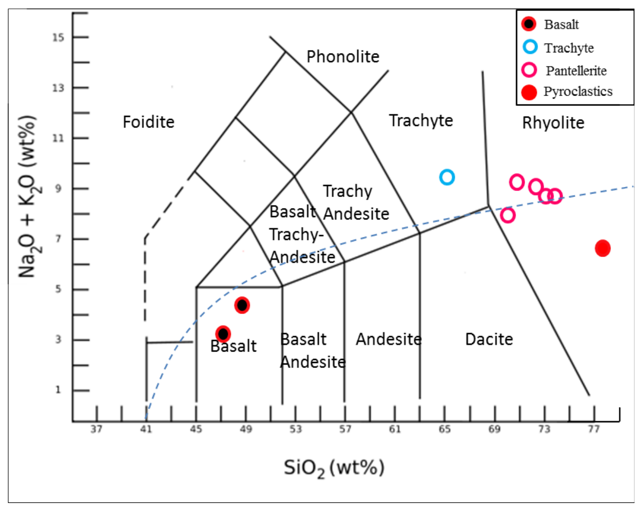

Figure 7. Alkali Silica classification diagram for the Eburru-Badlands samples. The curve is that of the alkaline - sub-alkaline boundary after Irvine and Baragar (1971).

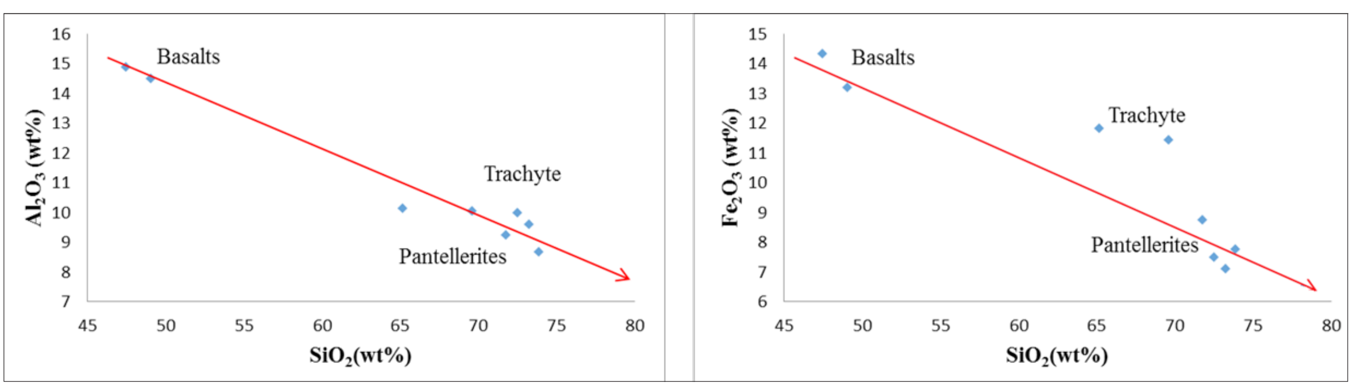

Figure 8. Major element (Al_2O_3 and Fe_2O_3) variation with SiO_2 for the Eburru-Badlands basalt, trachytes, and pantellerites. Arrows show the differentiation trend.

Geochemical data for the basalts and the silicic rocks suggests magmatic evolution via crystal fractionation from basalts (Weaver et al., 1975; Omenda, 1997; Beltran, 2003). This is evident from crystal fractionation showing a linear trend formed by basalts, trachytes and pantellerites in the TAS diagram. Other factors supporting this concept include the enrichment of incompatible trace elements in pantellerites relative to trachytes, the systematic depletion of the Rare Earth Elements (REE) from basalts through trachyte to pantellerites and the close spatial relation between trachytes and pantellerites from Eburru- Badlands area, (Figure 10).

Table 4. Trace element data for Eburru-Badlands samples.

Rock samples	2	8	13B	9	16	12	10	22	23
V	6	-2	3	301	347	1	2	2	0
Cr	4	4	4	52	43	3	6	8	5
Rb	132	173	115	25	10	258	235	83	179
Nb	335	400	179	39	29	264	352	359	321
Sr	4	4	17	459	478	10	12	27	4
Y	172	140	240	43	35	161	631	273	48
Zr	1749	2187	857	203	163	1758	1883	1807	1820
Co	4	6	6	16	16	7	10	5	6
Ni	9	7	0	38	48	7	13	11	8
Ba	66	42	46	474	653	10	39	149	49

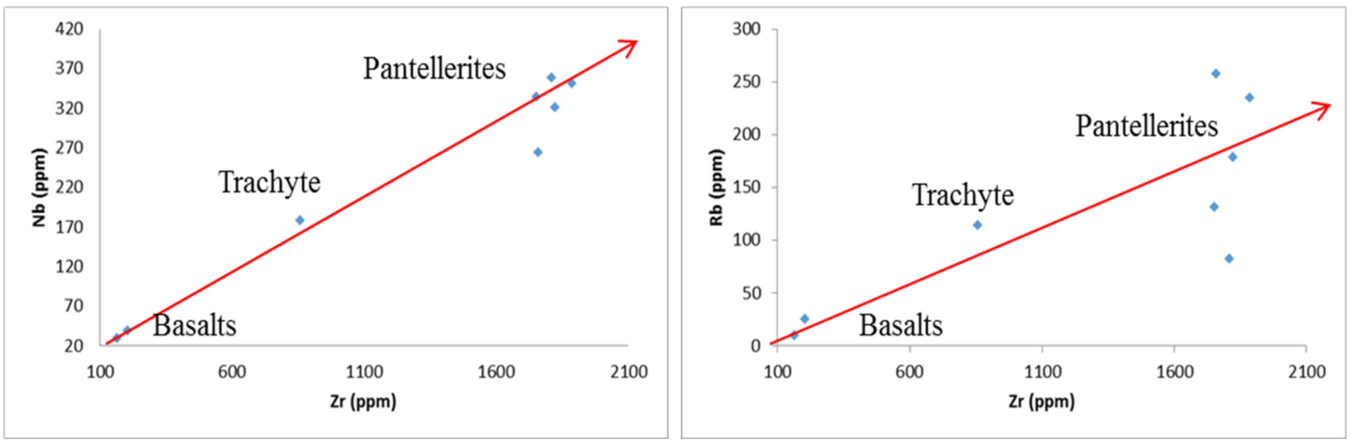

Figure 9. Incompatible element variation diagrams. The arrows indicate the trend of differentiation.

The variation in trace elements in the rock samples as shown in Table 4 displays a systematic increase in incompatible elements (Zr, Nb, Y and Rb) from basalts through trachyte to pantellerite, and decrease of compatible element concentrations (Co, Ni, Sr, Cr, V and Ba) indicating a close magmatic relationships between the rocks.

The TAS diagram shows that pantelleritic units are the most highly evolved rocks with high silica and high (Na_2O+K_2O) content hence strongly peralkaline. Silicic rocks are characterized by low Al_2O_3 and Fe_2O_3. Lower peralkalinity in basalts is associated with high Al_2O_3 with decrease in SiO_2. Analyzed basaltic and pyroclastic samples are subalkaline.

Major and trace element characteristics of peralkaline silicic rocks are most commonly interpreted to show that the magmas are mantle-derived mainly by fractionation of basaltic magmas.

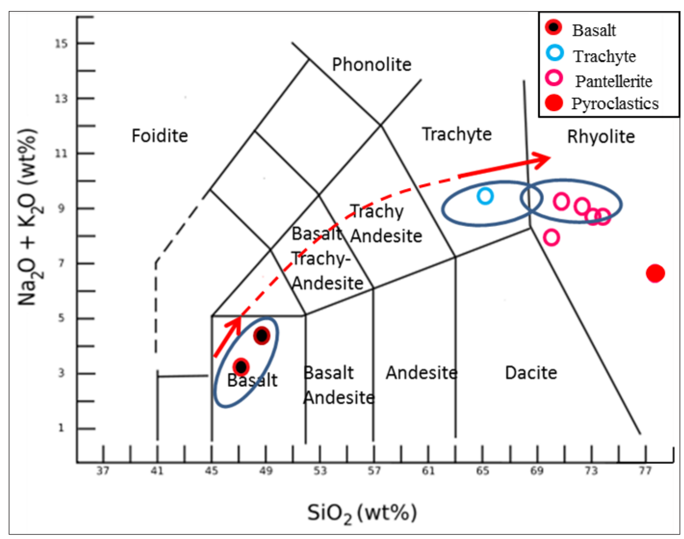

Figure 10. Evolutionary path with arrows showing generation of trachytes and pantellerites from parent basaltic lava.

By relating the occurrence of younger lavas influenced by the N-S faults, the open fractures forming mini-grabens and the geothermal manifestations along these faults, a good permeability trend can be modeled. These models will aid further exploration for geothermal resources in the Eburru-Badlands Geothermal Field.

6. References

Beltran, J. M.V., 2003: The origin of pantellerites and the geology of the Eburru volcanic complex, Kenyan rift, Africa. University of Texas at El Paso, Texas, USA, MSc. Thesis, 91 pp.

Clarke M. C. G., Woodhall D. G., Allen, D. and Darling, G., 1990: Geological, Volcanological and Hydrogeological controls on the occurrence of geothermal activity in the area surrounding Lake Naivasha, Kenya: Ministry of Energy, Kenya and British Geological Survey, Monograph, 138pp.

Irvine, T. N. and Baragar, W. R. A., 1971: A guide to the chemical classification of the common volcanic rocks. *Canadian Journal of Earth Science*, vol. 8, pp.523-548.

Kandie, R., 2014: Structural geology field mapping of the Eburru-Badlands geothermal prospect, KenGen internal report, 40 pp.

Le Bas, M. J., Le Maitre, R. W., Streckeisen, A. and Zanettin, B., 1985: A chemical classification of volcanic rocks based on the total alkali silica diagram. *Journal of Petrology*, vol. 27, pp.745-750.

Mariita, N.O., 2009: Exploration history of Olkaria geothermal field by use of geophysics. Short Course IV on Exploration for Geothermal Resources, organized by UNU-GTP, KenGen and GDC, Lake Naivasha, Kenya*,* 13 pp.

Omenda, P. A. and Karingithi, C.W., 1993: Hydrothermal model of Eburru Geothermal field, Kenya. Geothermal Resources Council, vol. 17, pp.155-160.

Omenda, P. A., 1997: The Geochemical Evolution of Quaternary Volcanism in the South - Central Portion of the Kenyan Rift. University of Texas at El Paso, Texas, USA, Doctoral dissertation, 218 pp.

Ren, M., Omenda, P.A., Anthony, E.Y., White, J.C., Macdonald, R. and Bailey, D.K., 2006: Application of the QUILF thermobarometer to the peralkaline trachytes and pantellerites of the Eburru volcanic complex, East African Rift, Kenya. *Lithos,* vol. 91, pp.109-204.

Weavers, D., Sceal, J. S. and Gibson I. L., 1972: Trace-element data relevant to the origin of trachytic and pantelleritic lavas in the East African Rift System: Contributions to Mineralogy and Petrology, vol. 36, pp.181-194.